Small mouse cholangiocytes proliferate in response to H1 histamine receptor stimulation by activation of the IP3/CaMK I/CREB pathway

Heather Francis, Shannon Glaser, Sharon DeMorrow, Eugenio Gaudio, Yoshiyuki Ueno, Julie Venter, David Dostal, Paolo Onori, Antonio Franchitto, Marco Marzioni, Shelley Vaculin, Bradley Vaculin, Khurshed Katki, Monique Stutes, Jennifer Savage and Gianfranco Alpini

Am J Physiol Cell Physiol 295:499-513, 2008. First published May 28, 2008;
doi:10.1152/ajpcell.00369.2007

Am J Physiol Cell Physiol 295: C499–C513, 2008.
First published May 28, 2008; doi:10.1152/ajpcell.00369.2007.

Small mouse cholangiocytes proliferate in response to H1 histamine receptor stimulation by activation of the IP_3/CaMK I/CREB pathway

Heather Francis,[3,4] Shannon Glaser,[2,4] Sharon DeMorrow,[2,4] Eugenio Gaudio,[6] Yoshiyuki Ueno,[7] Julie Venter,[2] David Dostal,[2,5] Paolo Onori,[8] Antonio Franchitto,[6] Marco Marzioni,[9] Shelley Vaculin,[1] Bradley Vaculin,[2] Khurshed Katki,[2] Monique Stutes,[4] Jennifer Savage,[2] and Gianfranco Alpini[1,2,3]

[1]*Central Texas Veterans Health Care System,* [2]*Department of Medicine and* [3]*Systems Biology and Translational Medicine,* [4]*Division of Research and Education,* [5]*Division of Molecular Cardiology, Scott & White and Texas A&M Health Science Center, College of Medicine, Temple, Texas;* [6]*Department of Human Anatomy, University of Rome, "La Sapienza," Rome;* [7]*Division of Gastroenterology, Tohoku University Hospital, Aobaku, Sendai, Japan;* [8]*Department of Experimental Medicine, State University of l'Aquila, l'Aquila; and* [9]*Department of Gastroenterology, Università Politecnica delle Marche, Ancona, Italy*

Submitted 16 August 2007; accepted in final form 21 May 2008

Francis H, Glaser S, DeMorrow S, Gaudio E, Ueno Y, Venter J, Dostal D, Onori P, Franchitto A, Marzioni M, Vaculin S, Vaculin B, Katki K, Stutes M, Savage J, Alpini G. Small mouse cholangiocytes proliferate in response to H1 histamine receptor stimulation by activation of the IP_3/CaMK I/CREB pathway. *Am J Physiol Cell Physiol* 295: C499–C513, 2008. First published May 28, 2008; doi:10.1152/ajpcell.00369.2007.—Cholangiopathies are characterized by the heterogeneous proliferation of different-sized cholangiocytes. Large cholangiocytes proliferate by a cAMP-dependent mechanism. The function of small cholangiocytes may depend on the activation of inositol trisphosphate (IP_3)/Ca^{2+}-dependent signaling pathways; however, data supporting this speculation are lacking. Four histamine receptors exist (HRH1, HRH2, HRH3, and HRH4). In several cells: *1*) activation of HRH1 increases intracellular Ca^{2+} concentration levels; and *2*) increased $[Ca^{2+}]_i$ levels are coupled with calmodulin-dependent stimulation of calmodulin-dependent protein kinase (CaMK) and activation of cAMP-response element binding protein (CREB). HRH1 agonists modulate small cholangiocyte proliferation by activation of IP_3/Ca^{2+}-dependent CaMK/CREB. We evaluated HRH1 expression in cholangiocytes. Small and large cholangiocytes were stimulated with histamine trifluoromethyl toluidide (HTMT dimaleate; HRH1 agonist) for 24–48 h with/without terfenadine, BAPTA/AM, or W7 before measuring proliferation. Expression of CaMK I, II, and IV was evaluated in small and large cholangiocytes. We measured IP_3, Ca^{2+} and cAMP levels, phosphorylation of CaMK I, and activation of CREB (in the absence/presence of W7) in small cholangiocytes treated with HTMT dimaleate. CaMK I knockdown was performed in small cholangiocytes stimulated with HTMT dimaleate before measurement of proliferation and CREB activity. Small and large cholangiocytes express HRH1, CaMK I, and CaMK II. Small (but not large) cholangiocytes proliferate in response to HTMT dimaleate and are blocked by terfenadine (HRH1 antagonist), BAPTA/AM, and W7. In small cholangiocytes, HTMT dimaleate increased IP_3/Ca^{2+} levels, CaMK I phosphorylation, and CREB activity. Gene knockdown of CaMK I ablated the effects of HTMT dimaleate on small cholangiocyte proliferation and CREB activation. The IP_3/Ca^{2+}/CaMK I/CREB pathway is important in the regulation of small cholangiocyte function.

heterogeneity; calcium; intrahepatic biliary epithelium; mitosis; transcription factors

THE INTRAHEPATIC BILIARY TREE is a three-dimensional network of interconnecting ducts of different sizes (with smaller ducts lined by smaller cholangiocytes and larger ducts lined by larger cholangiocytes) (2, 5, 11, 35, 47) and functions (2, 5, 35, 40–42, 44). In rat liver, large cAMP-responsive rat cholangiocytes express secretin receptor, cystic fibrosis transmembrane conductance regulator (CFTR), and Cl^-/HCO_3^- exchanger (2, 5) and secrete bicarbonate in bile by activation of cAMP, phosphorylation of protein kinase A (PKA), and opening of the Cl^- channel (CFTR), a series of events leading to activation of the Cl^-/HCO_3^- exchanger (2, 5, 34). The Cl^-/HCO_3^- exchanger has been identified recently as the Cl^-/HCO_3^- anion exchanger 2 (AE2) (10). In human liver, only medium bile ducts (that in rats have similar functional properties to large ducts) (2, 5, 7) express Cl^-/HCO_3^- AE2 (44). Although we have postulated (35, 46) that small rodent cholangiocytes may be primordial or undifferentiated cells, the function of small cholangiocytes is undefined.

In normal states, cholangiocytes are mitotically dormant (8) but proliferate in response to a number of pathological stimuli, including extrahepatic bile duct obstruction (BDL) (4, 8, 26, 52), α-naphthylisothiocyanate chronic feeding (42), sustained forskolin administration (21) or acute carbon tetrachloride (CCl_4) administration (40). The proliferative responses of cholangiocytes to these pathological maneuvers are heterogeneous and size-dependent (35). These findings have significant clinical relevance since human cholangiopathies selectively target different-sized bile ducts (38, 46). In rats, large but not small cholangiocytes selectively proliferate in response to BDL by activation of the cAMP system (3, 8). Although the activation of cAMP-dependent signaling is essential for the proliferation of large rat cholangiocytes (3, 21), it has been suggested (46) that the function of small cholangiocytes (that de novo proliferate following CCl_4-induced damage of large cholangiocytes and after chronic bile acid feeding) (6, 40, 42) may depend on the activation of the myo-D-inositol 1,4,5,trisphosphate (IP_3)/Ca^{2+}-dependent signaling pathway. However, this is conjectural since direct evidence for the role of this signaling pathway in the regulation of small cholangiocyte proliferation is lacking.

Histamine receptors, which are classified as HRH1, HRH2, HRH3, and HRH4, are expressed by a number of cells (50, 53). HRH1 exert their functions by coupling to $G_q\alpha$ mobilizing

Address for reprint requests and other correspondence: G. Alpini, Central Texas Veterans Health Care System, Scott & White and Texas A&M Health Science Center College of Medicine, Medical Research Bldg., 702 SW H.K. Dodgen Loop, Temple, TX, 76504 (e-mail: galpini@tamu.edu or galpini@medicine.tamhsc.edu).

The costs of publication of this article were defrayed in part by the payment of page charges. The article must therefore be hereby marked "*advertisement*" in accordance with 18 U.S.C. Section 1734 solely to indicate this fact.

intracellular Ca^{2+} concentration ($[Ca^{2+}]_i$) (15), whereas HRH2 is modulated by $G_s\alpha$ proteins coupled to adenylyl cyclase (49). Conversely, the HRH3/HRH4 couples to $G_{i/o}\alpha$ resulting in a negative regulation of cAMP (43). Because HRH1 exert their functions by coupling to $G_q\alpha$ mobilizing $[Ca^{2+}]_i$ (15), we hypothesized that activation of HRH1 modulates the proliferation of small cholangiocytes by a transduction pathway involving the activation of IP_3 and Ca^{2+}.

Ca^{2+}/calmodulin-dependent protein kinases or CaMK are serine/threonine-specific protein kinases that are primarily regulated by the Ca^{2+}/calmodulin complex (12, 29). CaMK I, II, and IV require Ca^{2+}/CaM binding and phosphorylation for activation (28). CaMK I and IV can phosphorylate the activating serine-133 (S133) residue of the cAMP-response element binding protein (CREB) (17, 57) and, in turn, stimulate CRE-mediated transcription. In support of the notion that CaMK regulates cholangiocyte functions, we have shown (45) that endogenous opioids modulate the growth of cholangiocytes in the course of cholestasis by an IP_3/CaMK II/protein kinase C (PKC)-α-dependent pathway. Furthermore, Ca^{2+}-dependent activation of Cl^- currents in the cholangiocarcinoma cell line Mz-ChA-1 is regulated by a CaMK II-dependent mechanism (48). No data exists regarding the role of CaMK in the modulation of small cholangiocyte proliferation.

We used immortalized cell lines of small and large murine cholangiocytes (61) that have been morphologically, phenotypically, and functionally characterized (61) and retain characteristics similar to that of freshly isolated small and large mouse cholangiocytes (25). Using this model, we evaluated: *1*) the expression of histamine receptor subtypes in small and large cholangiocytes and *2*) the role and intracellular mechanisms by which the specific HRH1 agonist histamine trifluoromethyl toluidide (HTMT) dimaleate (56) modulates the growth of immortalized small and large cholangiocytes.

MATERIALS AND METHODS

Materials

All reagents were obtained from Sigma Chemical (St. Louis, MO) unless otherwise indicated. Antibodies for secretin and histamine receptors and CaMK I, II, and IV were purchased from Santa Cruz Biotechnology (Santa Cruz, CA). The secretin receptor antibody (C-20) is an affinity-purified goat polyclonal antibody raised against a peptide mapping at the COOH terminus of secretin receptor of human origin. The CFTR monoclonal (IgG_1) antibody (M3A7; Thermo Fisher Scientific, Fremont, CA) was raised against the recombinant protein encoding the NBF2 domain of human CFTR. The anti Cl^-/HCO_3^- AE2 is an affinity-purified rabbit anti-rat AE2 IgG (no. AE21-A) that was purchased from Alpha Diagnostic International (San Antonio, TX). The HRH1 antibody (H-300) is a rabbit polyclonal antibody raised against amino acids 111-410 mapping near the COOH terminus of HRH1 of human origin. HRH2 (A-20) is an affinity-purified goat polyclonal antibody raised against a peptide mapping within an internal region of HRH2 of mouse origin. HRH3 (C-20) is an affinity-purified goat polyclonal antibody raised against a peptide mapping near the COOH terminus of HRH3 of human origin. HRH4 (C-20) is an affinity-purified goat polyclonal antibody raised against a peptide mapping within an internal region of HRH4 of human origin. CaMK I (M-20) is an affinity-purified goat polyclonal antibody (that detects all CaMK I subunits, α, β, δ, and γ) raised against a peptide mapping at the COOH terminus of CaMK I of mouse origin. CaMK II (M-176) is a rabbit polyclonal antibody (that detects all CaMK II subunits) raised against amino acids 303-478 mapping at the COOH terminus of CaMK II-α (Ca^{2+}/CaMK II, α, β, δ, and γ) of mouse origin. CaMK IV (M-20) is an affinity purified goat polyclonal antibody raised against a peptide mapping at the C-terminus of CaMK IV of mouse origin. All human antibodies cross-reacted with mouse.

The HRH1 agonist HTMT dimaleate (56) was purchased from Tocris Bioscience (Ellisville, MO). The intracellular Ca^{2+} chelator BAPTA/AM (23, 27), and W7 (a calmodulin antagonist that binds to calmodulin and inhibits Ca^{2+}/calmodulin-regulated enzyme activities such as CaMK protein kinase) (59) were obtained from Calbiochem (San Diego, CA). The RIA kits for the determination of intracellular cAMP (cAMP ^{125}I Biotrak Assay System, RPA509) and IP_3 (^3H Biotrak Assay System, TRK1000) levels were purchased from GE Healthcare (Piscataway, NJ).

Morphological, Phenotypic, and Functional Characterization of Immortalized Small and Large Murine Cholangiocytes

Small and large murine cholangiocytes isolated from normal mice (BALB/c) and immortalized by the introduction of the SV40 large-T antigen gene were previously established at the laboratory of Y. Ueno (61). The cell lines were maintained in minimum essential medium (Invitrogen, Carlsbad, CA) containing 10% heat-inactivated FBS, 1% penicillin and streptomycin, and 2 mmol/l L-glutamine at 37°C in a humidified 5% CO_2 incubator. We have previously shown that these cells display morphological (difference in size and transepithelial resistance) (61), phenotypic (expression of cytokeratin-19) (61), and functional features (cAMP response in large but not small cholangiocytes) (61) similar to freshly isolated small and large mouse (25) and rat (5, 7) cholangiocytes. We have performed additional experiments aimed to evaluate: *1*) the morphological appearance (by light microscopy) and cell size (by fluorescence-activated cell sorting or FACS) of immortalized small and large murine cholangiocyte lines and *2*) if immortalized small and large murine cholangiocytes are positive for cytokeratin-7 (CK-7, a cholangiocyte-specific marker) (26) but differentially express secretin receptor, CFTR, and Cl^-/HCO_3^- AE2, proteins that play important roles in the regulation of proliferative and secretory functions of large bile ducts (2, 3, 5, 7, 40, 41).

For light microscopy, trypsinized immortalized small and large cholangiocytes were smeared on slides, fixed in ice-cold acetone, allowed to air dry, and counterstained with 0.4% trypan blue. Images were obtained with an Olympus BX40 microscope equipped with an Olympus DP12 camera (Tokyo, Japan). Flow cytometry size determinations of cultured small and large cholangiocytes were performed on a BD FACSCalibur system using the CellQuest Pro software package (BD Biosciences, San Jose, CA). Before measurements, small and large cholangiocytes were diluted to 10^6 cells/ml in cell suspension buffer. Forty thousand events were recorded in each experiment. Cell sizes were estimated by comparing forward scatter (an index of cell size) signals with those of unstained polystyrene reference microspheres (5, 10, 15, and 20 μm; Polysciences, Warrington, PA) diluted in cell buffer at a concentration of 10^6 beads/ml. All of the bead standards had a relative refractive index (1.59 at 589 nm). Before sampling, the microspheres were uniformly suspended by mixing the suspensions.

Immunofluorescence for secretin receptor, CFTR, Cl^-/HCO_3^- AE2, and CK-7 was performed as follows. Immortalized small and large cholangiocytes were seeded on cover slips and allowed to adhere overnight. Cells were washed in 1× PBS containing 0.2% Triton X-100 (PBST), and blocked in 4% BSA (in PBST) for 1 h. The selected antibody was diluted (1:50) in 1% BSA/PBST, added to the cover slips, and incubated overnight at 4°C. Cells were washed three times for 10 min in PBST, and a 1:50 dilution (in 1% BSA/PBST) of cy3-conjugated anti-rabbit secondary antibody (Jackson Immunochemicals, West Grove, PA) was added for 2 h at room temperature. Cells were washed again and mounted on microscope slides with Antifade gold containing 4,6-diamidino-2-phenylindole (DAPI) as a nuclear stain (Molecular Probes, Eugene, OR). Negative controls were

performed by usage of a preimmune serum in the place of the primary antibody. Staining was visualized using an Olympus IX-71 inverted confocal microscope.

Isolation of Small and Large Normal Mouse Cholangiocytes

Because the size of isolated small and large normal mouse cholangiocytes (25) is similar to that of small and large purified rat cholangiocytes (5), we have used similar parameters (5) for the isolation of these cells. Following standard collagenase perfusion, a mixed nonparenchymal cell fraction was separated into two distinct subpopulations of small and large cholangiocytes by centrifugal elutriation (2,500 revolutions/min at the flow rates of 22 and 70 ml/min, respectively) using a Beckman J2–21M centrifuge equipped with a JE-6B rotor (Beckman Instruments, Fullerton, CA) (5). Small and large cholangiocytes were further purified by a monoclonal antibody, rat IgG_{2a} (provided by Dr. R. Faris, Providence, RI), against an antigen expressed by mouse cholangiocytes (26). Cell number and viability were assessed by trypan blue exclusion. The size of the two subpopulations of cholangiocytes was evaluated by FACS analysis.

Expression of Histamine Receptor

HRH1 receptor expression was determined by *1*) immunohistochemistry in normal mouse liver sections and *2*) immunofluorescence, immunohistochemistry, and immunoblots in immortalized small and large cholangiocytes. Real-time PCR was used to further confirm the presence of HRH1 in freshly isolated small and large cholangiocytes and immortalized small and large cholangiocytes. Furthermore, we evaluated the expression of HRH2, HRH3, and HRH4 in *1*) liver sections by immunohistochemistry and *2*) small and large immortalized cholangiocytes by real time PCR.

Immunohistochemistry

Normal mouse liver sections (4 μm) and cell smears of immortalized small and large cholangiocytes (fixed in Bouin solution) were mounted on glass slides coated with acetone aminopropyltriehoxylan (2%) solution. After deparaffination, endogenous peroxidase activity was blocked by incubation (30 min) in methanolic hydrogen peroxide (2.5%). Sections were hydrated in graded ethanol and rinsed in 1× PBS. The endogen biotin was blocked by the Biotin Blocking System (Dako Cytomation, Glostrup, Denmark). Following washes in 1× PBS, sections were incubated overnight at 4°C with antibodies for HRH1, HRH2, HRH3, or HRH4 (1:100 dilution), whereas cell smears were incubated with HRH1 antibody (1:100 dilution). Samples were rinsed with 1× PBS, incubated for 10 min at room temperature with a secondary biotinylated antibody (Dako Cytomation LSAB Plus System-HRP) and then with Dako ABC (Dako Cytomation LSAB Plus System-HRP), developed with 3–3′ diaminobenzidine, and counterstained with hematoxylin. For all immunoreactions, negative controls (preimmune serum substituted for primary antibody) were included. Observations and light microscopy photographs of liver sections were taken by Leica Microsystems DM 4500 B Light Microscopy (Weltzlar, Germany) with a Jenoptik Prog Res C10 Plus Videocam (Jena, Germany).

Immunofluorescence

Immunofluorescence for HRH1 in immortalized small and large murine cholangiocyte lines was performed as described above for secretin receptor, CFTR, and Cl^-/HCO_3^- AE2 with the exception that an antibody (1:10 dilution) specific for HRH1 was used. Following incubation with HRH1 antibody, cells were washed three times for 10 min in PBST, and a 1:50 dilution (in 1% BSA/PBST) of cy3-conjugated anti-rabbit secondary antibody (Jackson Immunochemicals) was added for 2 h at room temperature. Cells were washed again and mounted on microscope slides with Antifade gold containing DAPI as a nuclear stain. Negative controls were performed by usage of a preimmune serum in the place of the primary antibody. Staining was visualized using an Olympus IX-71 inverted confocal microscope.

Real-Time PCR

We evaluated the expression of: *1*) HRH1 mRNA in total RNA (1.0 μg) from immortalized small and large murine cholangiocytes and freshly isolated small and large normal mouse cholangiocytes and *2*) HRH2, HRH3, and HRH4 in immortalized small and large cholangiocytes by using the RT^2 Real-Time assay from SuperArray (Frederick, MD), an approach we have previously used to evaluate the expression of HRH3 in purified rat cholangiocytes (20). cDNA template (1 μl) was added to 12.5 μl of master mix, 10.5 μl of deionized water, and 1 μl of RT^2 PCR mouse primers (SuperArray) designed specifically for the messages for HRH1, HRH2, HRH3, and HRH4 and glyceraldehyde-3-phosphate dehydrogenase (GAPDH), the housekeeping gene (3, 20). A $\Delta\Delta C_T$ (delta delta of the threshold cycle) analysis was performed using the normal pooled cholangiocytes as the control sample. Data were expressed as relative mRNA levels ± SE of HRH1 to GAPDH ratio ($n = 3$).

Immunoblotting

Immunoblotting analysis for HRH1 was performed as described (23) in protein (10 μg) from brain (positive control) or whole cell lysate that was harvested from immortalized small and large murine cholangiocytes by sonication (6 times in 30-s bursts) in RIPA buffer [50 mmol/l Tris, pH 7.5, 150 mmol/l NaCl, 1% Nonidet P-40 (NP-40), 0.5% deoxycholic acid, 0.1% SDS, 2 mmol/l EDTA, 10 mmol/l NaF, 10 μg/ml leupeptin, 20 μg/ml aprotinin, and 1 mmol/l phenylmethylsulfonyl fluoride]. After stripping, the amount of protein loaded was normalized by immunoblots for β-actin (6). The intensity of the bands was determined by scanning video densitometry using the phospho-imager, Storm 860, (GE Healthcare) and the ImageQuant TL software version 2003.02 (GE Healthcare, Little Chalfont, Buckinghamshire, UK).

Effect of HTMT Dimaleate on the Proliferation of Immortalized Small and Large Cholangiocytes

The proliferation of immortalized small and large cholangiocytes was evaluated by the CellTiter 96 AQueous One Solution Cell Proliferation Assay (Promega, Madison, WI) (18) that uses a novel tetrazolium compound, 3-(4, 5-dimethylthiazol-2-yl)-5-(3-carboxymethoxyphenyl)-2-(4-sulfophenyl)-2H-tetrazolium, inner salt, in combination with an electron coupling reagent, phenazine ethosulfate, to produce a colorimetric change. Absorbance was measured at 490 nm on a microplate spectrophotometer (Versamax; Molecular Devices, Sunnyvale, CA). Data were expressed as the degree of change of treated cells compared with vehicle-treated controls. After trypsinization, immortalized small and large cholangiocytes were seeded in 96-well plates (10,000/well) in a final volume of 200 μl of medium. Subsequently, cells were stimulated for 24 and 48 h with HTMT dimaleate (10 μM) (56) before evaluation of proliferation by CellTiter Assay. In different sets of experiments, immortalized small cholangiocytes were stimulated for 48 h with: *1*) HTMT dimaleate (10 μM) in the absence or presence of preincubation (1 h) with BAPTA/AM (an intracellular Ca^{2+} chelator, 1 μM) (51), W7 (a calmodulin antagonist, 10 μM), (54), or terfenadine (a specific HRH1 inhibitor, 5 μM) (33); or *2*) histamine (1 μM) in the absence or presence of terfenadine (5 μM).

To exclude the role of CaMK II in HTMT dimaleate-induced increase in small cholangiocyte growth, we evaluated the effect of HTMT dimaleate in small cholangiocytes in the absence or presence of the highly-specific CaMK II inhibitor autocamtide-2-related inhibitory peptide (AIP) (30, 31) that at the concentration used (1 μM) completely inhibits CaM kinase II but does not affect PKC, PKA, CaMK I, CaMK IV, and other brain extract kinases (9, 31).

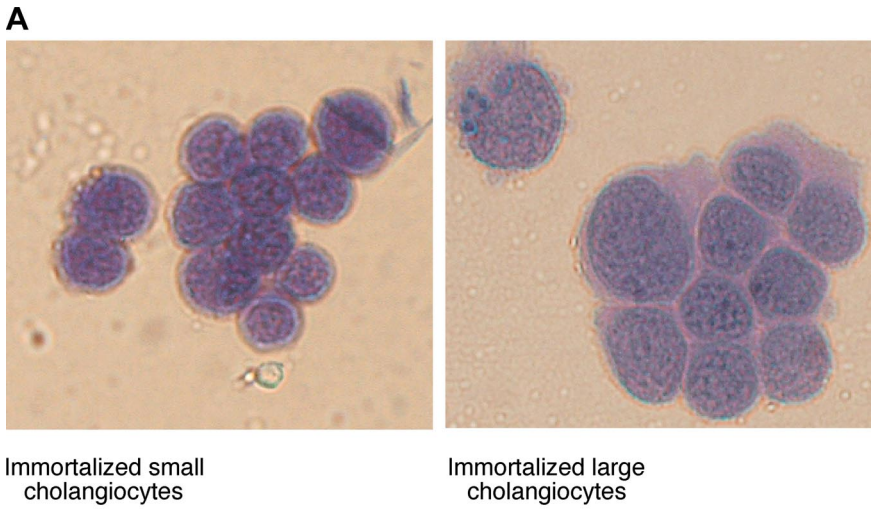

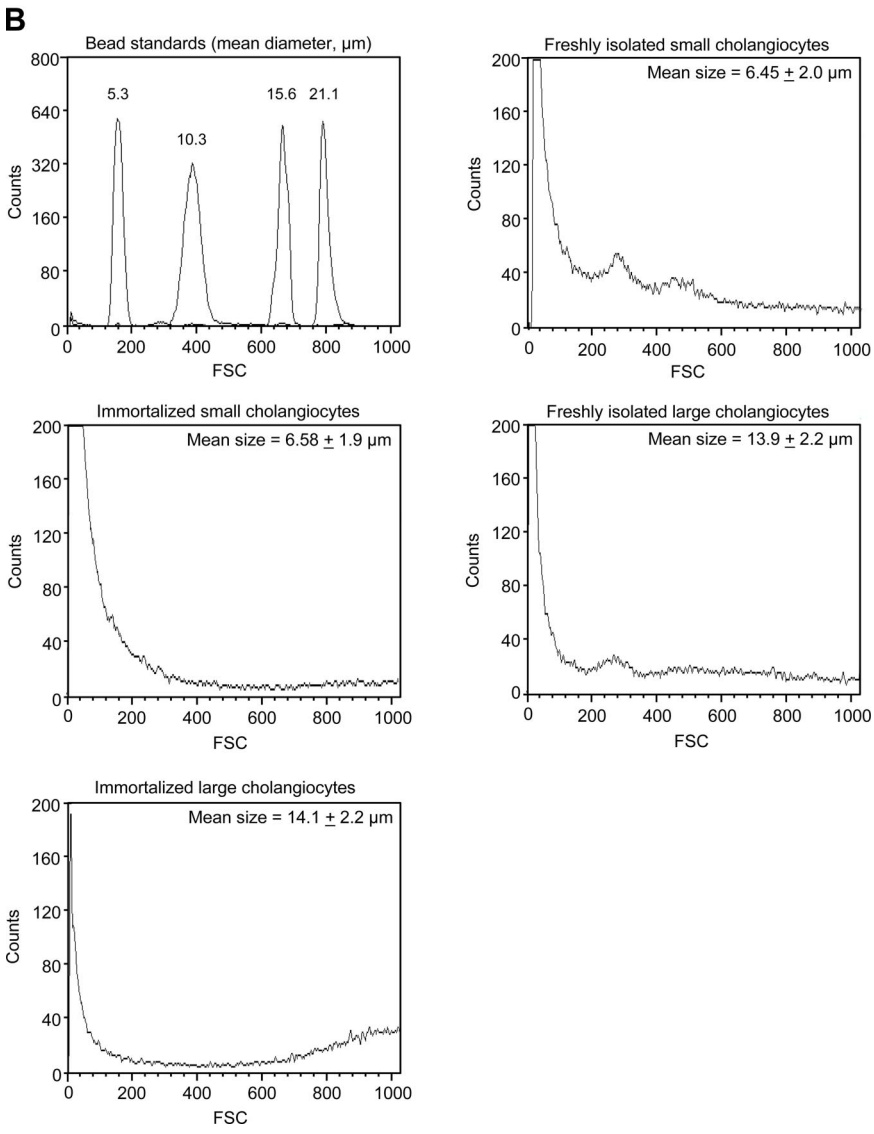

Fig. 1. *A*: light micrographs of immortalized small and large murine cholangiocytes. These two cell subtypes differ in morphological appearance and diameter. Original magnification ×400. *B*: size profiles of small and large cholangiocytes. Forward scatter (FSC) profiles were performed on immortalized and freshly isolated small and large cholangiocytes. The average cell diameter in each population was determined by comparing mean FSC signal with those of unstained microsphere size standards. FSC profiles of the microsphere standards are shown in *top left*. The average diameter (in μm) provided by the manufacturer is given above each peak. Cell sizes were calculated using a regression line constructed from mean FSC profiles of the standards. Means ± SE of FSC signals shown in histograms were determined using BD CellQuest Pro software, in which 40,000 events were recorded for each sample. *C*: representative immunofluorescent micrographs of immortalized small and large cholangiocytes stained for secretin receptor (SR), cystic fibrosis transmembrane conductance regulator (CFTR), Cl^-/HCO_3^- anion exchanger 2 (Cl^-/HCO_3^- AE2), and cytokeratin-7 (CK-7). Corresponding negative controls are included. Bar = 50 μm.

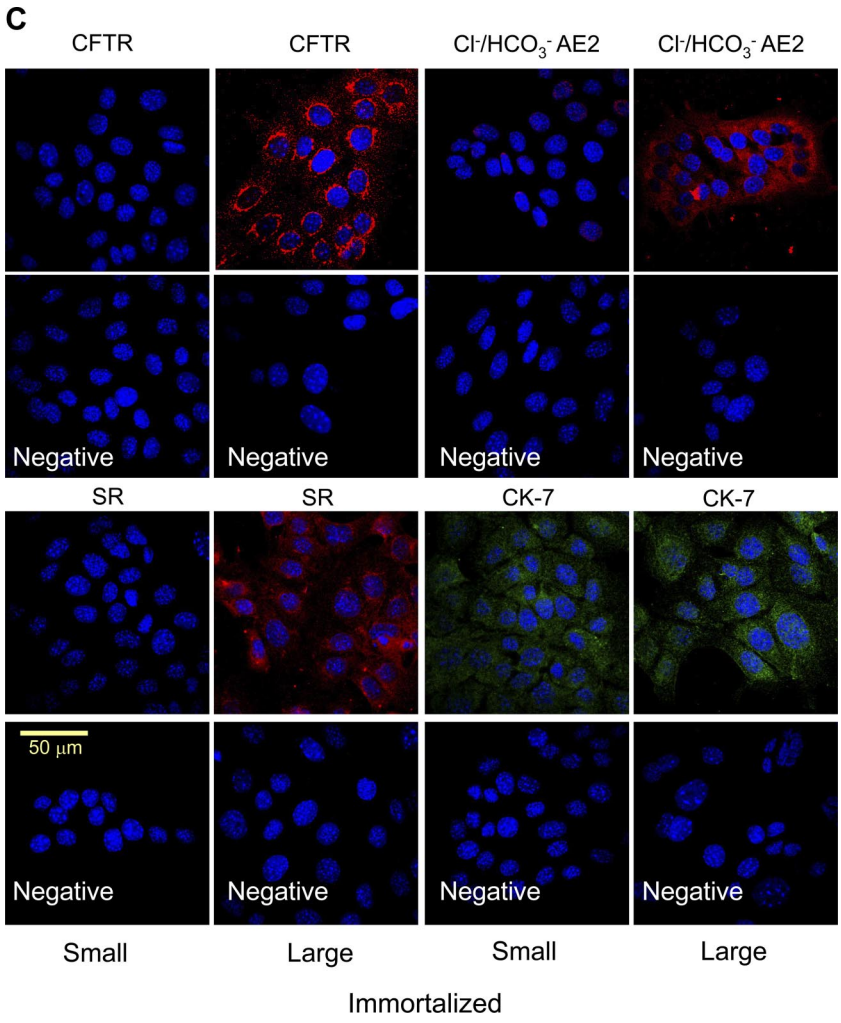

Fig. 1 —*Continued*

Evaluation of the Intracellular Mechanisms of HRH1 Modulation of Small Cholangiocyte Proliferation

Measurement of IP_3, Ca^{2+}, and cAMP levels. The effects of HTMT dimaleate on the intracellular levels of: *1*) IP_3 in immortalized small and large cholangiocytes and *2*) cAMP in immortalized small cholangiocytes were evaluated by commercially available RIA kits (2, 3, 5, 21, 37, 39) according to the vendors' instructions. After trypsinization, immortalized cholangiocytes were washed with 1× Hanks' balanced salt solution (1× HBSS), incubated for 1 h at 37°C (21, 23, 37) to regenerate membrane proteins damaged by trypsinization (32), and stimulated at room temperature with 0.2% BSA (basal) or HTMT dimaleate (10 μM) for 10 min (39) before measurement of IP_3 levels and 5 min (2, 3, 5, 21, 37, 39) before cAMP evaluation (2, 3, 5, 21, 37, 39). $[Ca^{2+}]_i$ fluorescence measurements in immortalized small cholangiocytes were performed using fluo 3-AM (Molecular Probes) and a Fluoroskan Ascent FL (ThermoLabsystems, Helsinki, Finland) microplate reader equipped with three injectors as described in detail (19, 22, 36, 58). Small cholangiocytes (4×10^4/well) were loaded for 1 h at room temperature with 5 μM of fluo 3-AM in 1× HBSS with 0.1% Pluronic F-127 (Molecular Probes). After washes with 1× HBSS, the loaded cells were added to a 96-well black microplate. The baseline fluorescence was measured 50 times after 1 s at 2-s intervals; 1× HBSS alone or HTMT dimaleate (10 μM) dissolved in buffer was injected sequentially in separate wells, and the fluorescence intensity was measured at 538 nm for 3 min at 1-s intervals. The excitation wavelength was 485 nm. $[Ca^{2+}]_i$ was calculated as follows: $[Ca^{2+}]_i = K_d(F - F_{min})/(F_{max} - F)$. F_{max} refers to fluorescence intensity measured after permeabilization of the cells with 1% NP-40, and F_{min} is the minimum fluorescence. Next, 0.1 M EGTA (pH 8.0) was added to chelate Ca^{2+}, and F_{min} was obtained. Ionomycin (a Ca^{2+} ionophore, 10 μM) (58) was used at the end of each Ca^{2+} determination to ensure cholangiocyte responsiveness.

Role of CaMK Isoforms in HTMT Dimaleate Modulation of Cholangiocyte Proliferation

We first evaluated: *1*) the protein expression of CaMK I, CaMK II, and CaMK IV in normal mouse liver sections by immunohistochemistry and *2*) protein and message expression of CaMK I and CaMK II (the two isoforms expressed by bile ducts in liver sections) in immortalized small and large cholangiocytes by immunoblots and real-time PCR, respectively (23).

We evaluated, by semiquantitative immunohistochemistry of paraffin-embedded serial liver sections (4 μm), the number of cholangiocytes positive for CaMK I, CaMK II, and CaMK IV. Immunohistochemistry was performed as described above for staining of histamine receptors with the exception that the antibodies specific for the CaMK isoforms were used. The data were obtained from the cumulative evaluation of 10 different fields from three different sections.

Immortalized small and large cholangiocytes were lysed as described above, and 10 μg of protein were used to determine the expression of CaMK I and CaMK II by immunoblotting using antibodies against the two isoforms. Following stripping, β-actin was

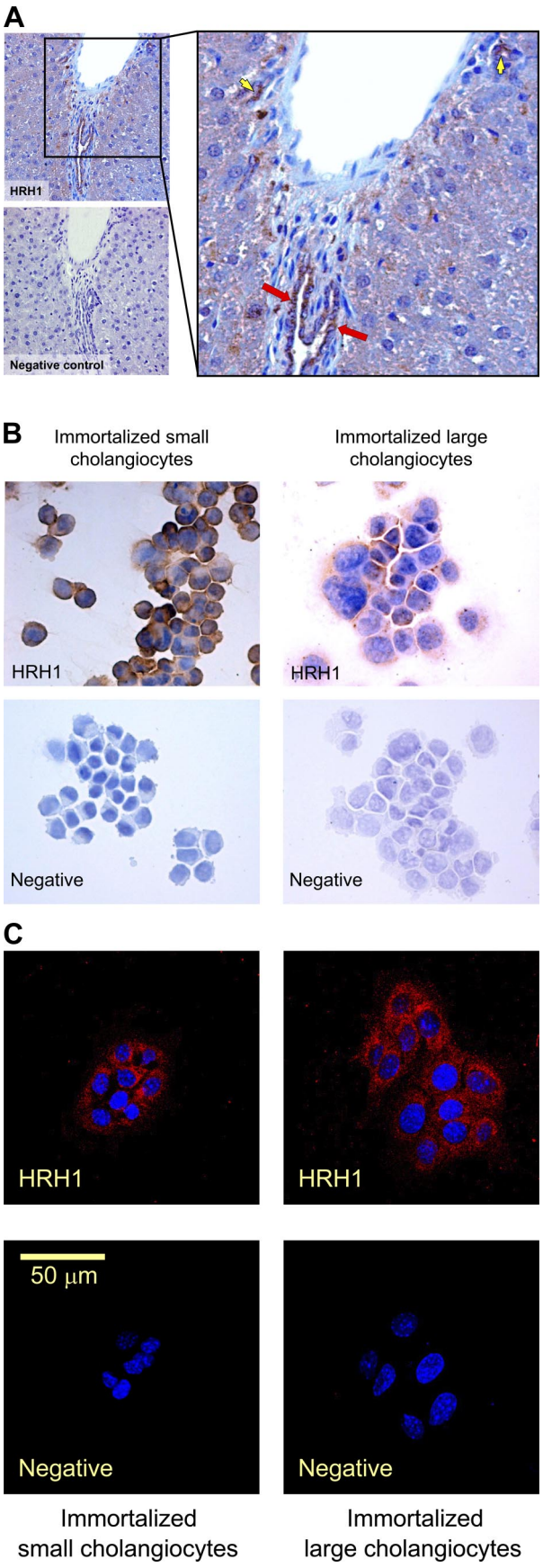

used for normalization of the amount of proteins used (6). The intensity of the bands was quantified as described above.

Real-time PCR for CaMK I-α, -γ, and -δ and CaMK II-α, -γ, and -δ in immortalized small and large murine cholangiocytes was performed as described above for histamine receptors using primers from SuperArray.

We next evaluated the effect of HTMT dimaleate on the phosphorylation of CaMK I in immortalized small cholangiocytes. Briefly, 1×10^6 cholangiocytes were seeded in six-well plates and allowed to grow overnight to ~80% confluence. Subsequently, cells were stimulated with 0.2% BSA (basal) or HTMT dimaleate (10 μM) for 24 h. The relative levels of phosphorylated CaMK I were determined in protein (10 μg) from whole cell lysate by immunoblotting. After being stripped, immunoblots were normalized with the protein for total CaMK. The intensity of the bands was quantified as described above.

Role of CaMK I in HRH1 Modulation of Small Cholangiocyte Proliferation

To further confirm the role of CaMK I in HRH1 modulation of small cholangiocyte proliferation, we used short hairpin RNA (shRNA) to develop a stable transfected cell line. Knockdown of the CaMK I gene was performed using a SureSilencing shRNA (SuperArray) plasmid for mouse CaMK I containing the gene for neomycin (geneticin; Invitrogen) resistance for the selection of transfected cells, according to the instructions provided by the vendor. Briefly, immortalized small cholangiocytes were transfected with either CaMK I shRNA or the empty shRNA vector in a six-well plate with Mirus *Trans*IT-LT1 Transfection Reagent. Transfected cells were selected by the addition of 500 μg/ml of neomycin in the media, and the selection process was allowed to continue for 3–4 days. Surviving cells were then split to a lower density in a 12-well plate so that each clone stems from only 5–10 cells. A total of 24 clones was then assessed for the relative knockdown of CaMK I using real-time PCR (as described above), and a single clone with the greatest degree of knockdown was selected for subsequent experiments. After establishing knockdown efficiency (~70%), small cholangiocyte proliferation was evaluated by CellTiter Assay after stimulation with 0.2% BSA or HTMT dimaleate (10 μM) for 48 h.

Pharmacologic and Genetic Manipulation of CREB Activation

We evaluated the role of HRH1 and CaMK I on CREB activation by using the TransAM pCREB Transcription Factor Assay Kit from Active Motif. The kit was performed according the directions provided by the vendor. Nuclear extracts were obtained using the Nuclear Extraction Kit from Active Motif. In pharmacological experiments, nuclear extracts were prepared from immortalized small cholangiocytes stimulated for 48 h at 37°C with 0.2% BSA (basal) or HTMT dimaleate (10 μM) in the absence or presence of preincubation with W7 (10 μM) in serum-free conditions. For genetic manipulation of CaMK I-dependent CREB activity, we used the CaMK I knockdown cell line (described above) to obtain nuclear extracts. Knockdown and empty vector cells were plated and stimulated with 0.2% BSA (basal) or HTMT dimaleate (10 μM) for 48 h. The assay was performed as

Fig. 2. *A*: immunohistochemistry for histamine receptor (HRH) 1 in normal mouse liver sections shows that small (yellow arrowheads) and large (red arrows) bile ducts are positive for this receptor. Low magnification ×10; high magnification of the same field, ×40. *B*: immunohistochemistry for HRH1 in immortalized small and large murine cholangiocytes. Original magnification ×40. *C*: immunofluorescence for HRH1 in smears of immortalized small and large murine cholangiocytes. Bar = 50 μm. *D*: real-time PCR for: *1*) HRH1, HRH2, HRH3, and HRH4 mRNAs in total RNA (1.0 μg) from immortalized small and large cholangiocytes and *2*) HRH1 mRNA in total RNA (1.0 μg) from freshly isolated small and large cholangiocytes from normal mice. Data are means ± SE of 3 experiments. $^*P < 0.05$ vs. large cholangiocytes. *E*: immunoblotting analysis for the HRH1 in protein (10 μg) from whole cell lysate from immortalized small and large cholangiocytes. Data are means ± SE of 3 experiments. $^*P < 0.05$ vs. large cholangiocytes.

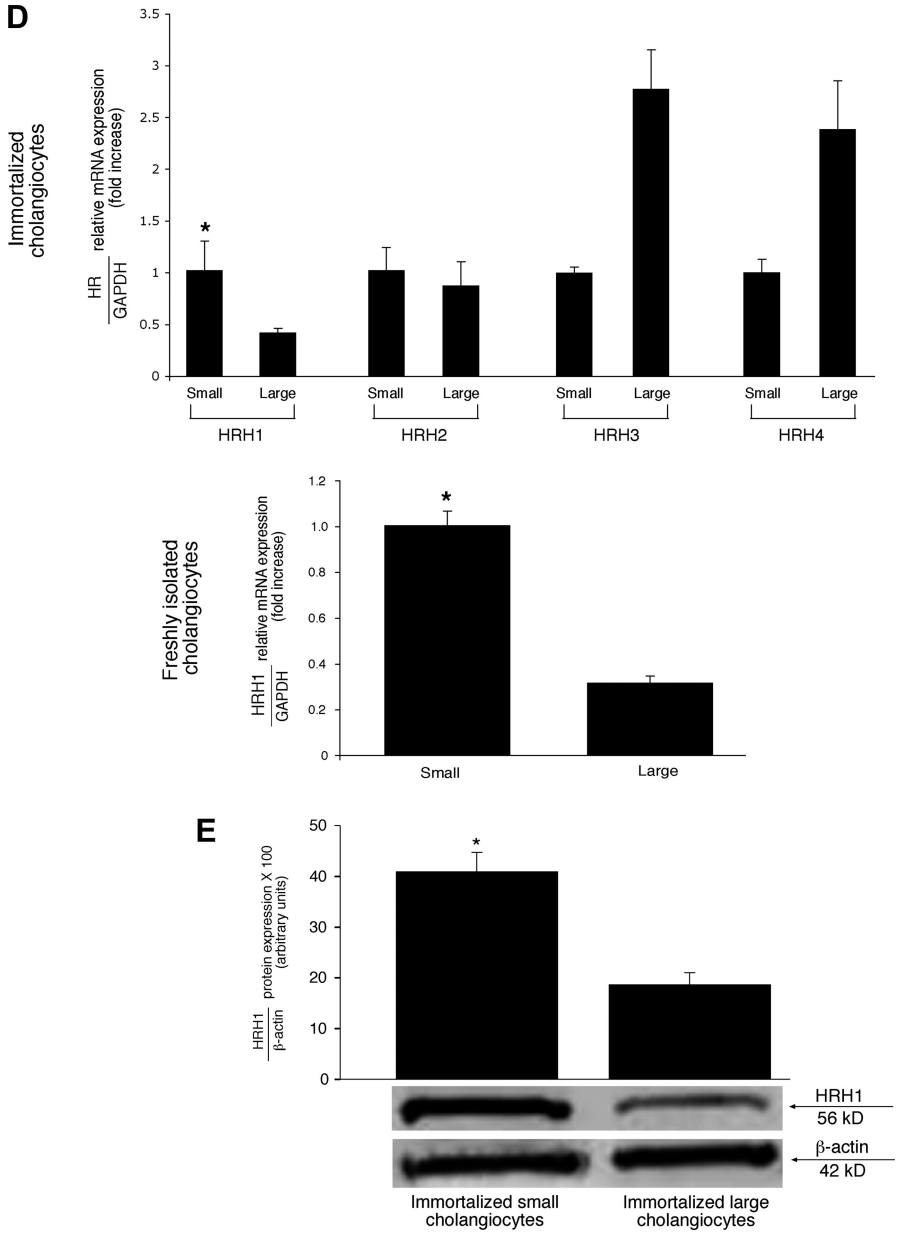

Fig. 2 —*Continued*

follows. Nuclear extracts were plated on a precoated 96-well plate with 30 μl of complete binding buffer. Nuclear extracts were incubated for 3 h at room temperature on a rocking platform. After careful washing, 100 μl of phospho-CREB antibody (1:500 dilution in 1× antibody binding buffer) were added to all wells. The plate was incubated for 1 h at room temperature. Wells were washed three times, and 100 μl of diluted HRP antibody (1:100 dilution in 1× antibody binding buffer) were added to each well and incubated for 1 h at room temperature. After washing (4 times), 100 μl of developing solution was added to all wells, and the plate was incubated for 10 min at room temperature protected from light. Stop solution (100 μl) was added, and the plate was read within 5 min at 450 nm. Data were determined as a degree of increase over basal values.

Statistical Analysis

All data are expressed as means ± SE. The differences between groups were analyzed by Student's *t*-test when two groups were analyzed or ANOVA if more than two groups were analyzed. A P value <0.05 was used to indicate statistically significant differences.

RESULTS

Morphological and Functional Characterization of Immortalized Small and Large Cholangiocytes

We demonstrated that immortalized small and large cholangiocytes differ in morphological appearance (by light microscopy, Fig. 1*A*) and size (by FACS analysis, Fig. 1*B*). Forward scatter profiles revealed that small and large cholangiocytes were heterogeneous in size (Fig. 1*B*). When cells were compared using microsphere size standards (5–20 μm), mean diameters of immortalized and freshly isolated small cholangiocytes were similar (Fig. 1*B*). Likewise, mean diameters of immortalized and freshly isolated large cholangiocytes were similar (Fig. 1*B*). Mean diameters of cells in small and large populations were significantly different ($P < 0.001$) for both immortalized and freshly isolated cholangiocytes (Fig. 1*B*). Large immortalized (but not small) cholangiocytes expressed

secretin receptor, CFTR, and Cl^-/HCO_3^- AE2 (Fig. 1*C*). Immortalized small and large cholangiocyte lines were positive for CK-7 (Fig. 1*C*). The corresponding negative controls are shown in Fig. 1*C*.

Evaluation of Histamine Receptor Expression in Liver Sections and Small and Large Cholangiocytes

In normal mouse liver sections, both small and large bile ducts expressed HRH1 (Fig. 2*A*), and HRH2, HRH3, and HRH4 (not shown). By immunohistochemistry (Fig. 2*B*) and immunofluorescence (Fig. 2*C*), immortalized small and large cholangiocytes expressed HRH1. By real-time PCR, immortalized small and large cholangiocytes, and freshly isolated small and large cholangiocytes, expressed HRH1 mRNA (expressed as a ratio to GAPDH mRNA, Fig. 2*D*). In both immortalized and freshly isolated small and large cholangiocytes, message levels were higher in small cholangiocytes compared with large cholangiocytes (Fig. 2*D*). By real-time PCR, we have also shown that immortalized small and large cholangiocyte lines express HRH2, HRH3, and HRH4 messages (Fig. 2*D*). Similar to the real-time PCR results, the protein expression of HRH1 was higher in immortalized small cholangiocytes compared with large cholangiocytes (Fig. 2*E*). The expression of β-actin, which was used to normalize the amount of protein loaded (6), was similar between small and large cholangiocytes (Fig. 2*E*).

Effect of HTMT Dimaleate on Small and Large Cholangiocyte Proliferation

By CellTiter Assay, we demonstrated that the proliferation of immortalized small (but not large) cholangiocytes increases (compared with basal treatment) ~40 and 50%, respectively, after HRH1 stimulation for 24 and 48 h (Fig. 3*A*). The stimulation of small cholangiocyte proliferation by HTMT dimaleate was blocked by the HRH1 antagonist terfenadine (33), the intracellular Ca^{2+} chelator BAPTA/AM (51), and the calmodulin antagonist W7 (59), but not by the highly-specific CaMK II inhibitor AIP (30, 31) (Fig. 3*B*). Terfenadine, BAPTA/AM, W7, or AIP alone did not change the proliferation of small cholangiocytes (not shown). Histamine stimulation of small cholangiocyte proliferation was prevented by preincubation with terfenadine (Fig. 3*B*).

Effect of HTMT Dimaleate on Intracellular IP_3, Ca^{2+}, and cAMP Levels

HTMT dimaleate increased IP_3 levels of immortalized small (but not large) murine cholangiocytes compared with small cholangiocytes treated with 0.2% BSA (basal) (Fig. 4*A*). HTMT dimaleate did not change intracellular cAMP levels of immortalized small cholangiocytes compared with their corresponding basal values (Fig. 4*B*).

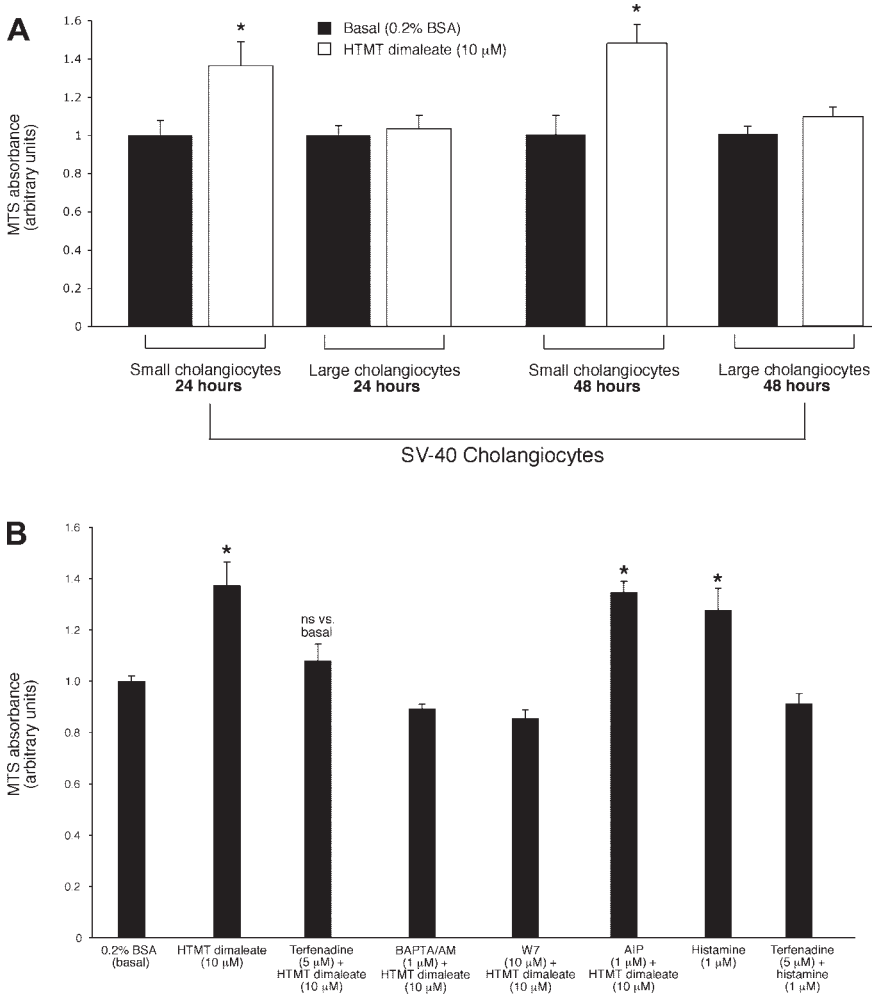

Fig. 3. *A*: effect of histamine trifluoromethyl toluidide (HTMT dimaleate) (10 μM for 24 and 48 h) on the proliferation of immortalized small and large cholangiocytes. Data are means ± SE of 10 experiments. *$P <$ 0.05 vs. its corresponding basal value. *B*: effect of *1*) HTMT dimaleate (10 μM for 48 h) in the absence or presence of terfenadine (5 μM), BAPTA/AM (1 μM), W7 (10 μM), and AIP (1 μM) or *2*) histamine (1 μM for 48 h) in the absence or presence of terfenadine (5 μM). Data are means ± SE of 8 experiments. *$P < 0.05$ vs. its corresponding basal value.

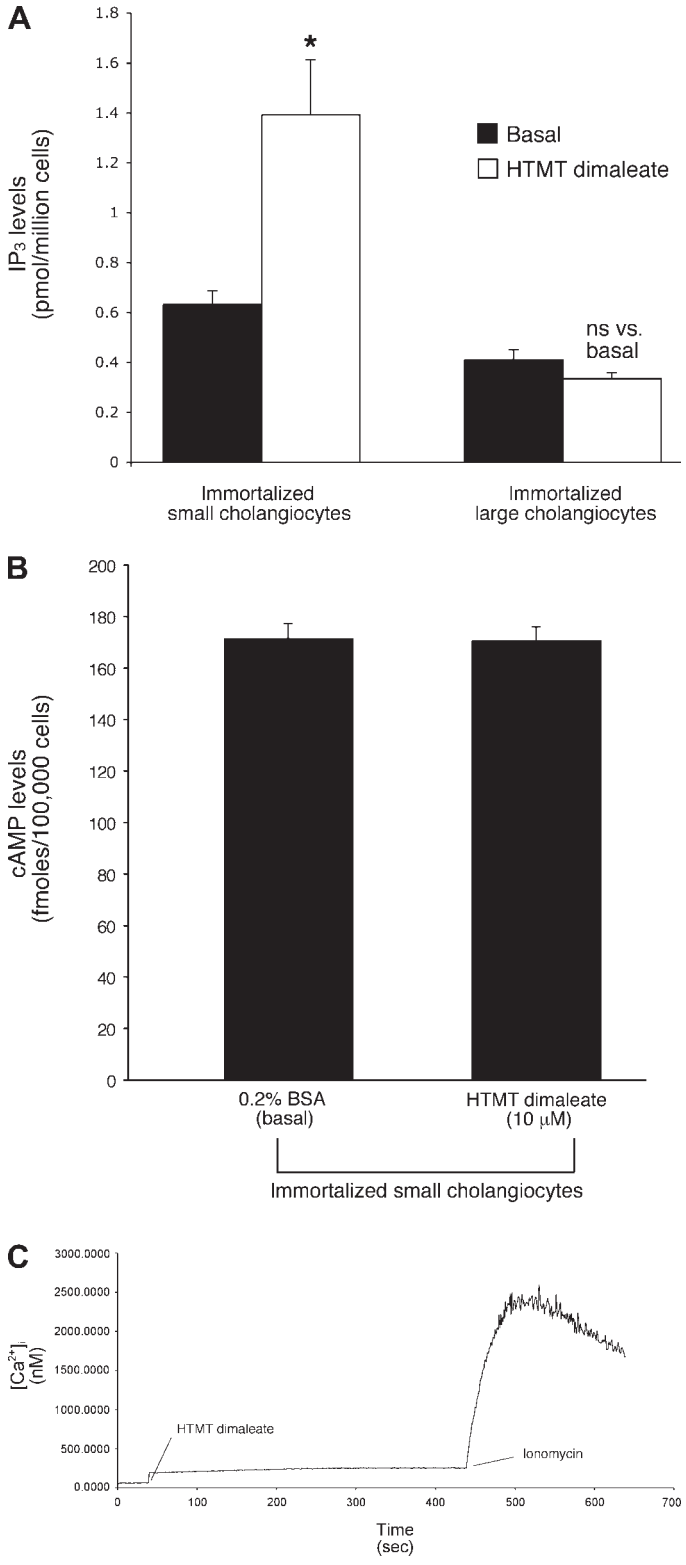

Fig. 4. Effects of 0.2% BSA (basal) or HTMT dimaleate (10 μM) on IP_3 synthesis (10 min incubation) in immortalized small and large cholangiocytes (*A*) or cAMP levels (5 min incubation) in immortalized small cholangiocytes (*B*). Data are means ± SE of 6 experiments. *$P < 0.05$ vs. corresponding basal levels. *C*: average measurement of $[Ca^{2+}]_i$ levels ($n = 3$) in immortalized small cholangiocytes under basal conditions (0.2% BSA) at the start and following treatment with 10 μM HTMT dimaleate (10 min treatment). The effect of the addition of the Ca^{2+} ionophore ionomycin (10 μM) on intracellular Ca^{2+} concentration ($[Ca^{2+}]_i$) levels in small cholangiocytes is shown as indicated.

HTMT dimaleate increased $[Ca^{2+}]_i$ levels in small cholangiocytes compared with small cholangiocytes treated with 0.2% BSA (Table 1 and Fig. 4*C*). In agreement with our previous studies (1, 19, 39), Ca^{2+} dynamics of small cholangiocytes (following stimulation with HTMT dimaleate) were slower and not characterized by a Ca^{2+} spike (Fig. 4*C*). The method that we used (19, 22) results in Ca^{2+} measurements, which are an average signal of 400,000 cells rather than typical single cell measurements (1, 19, 39). This approach gives us similar data to that obtained with measurements that were made in single cells loaded with fluo 3-AM (1, 19, 39).

Role of CaMK Isoforms in HTMT Dimaleate Modulation of Small Cholangiocyte Proliferation

By semiquantitative immunohistochemistry in serial liver sections from normal mice, we have shown that both small and large bile ducts were positive for CK-7 (Fig. 5*A*) and CaMK I and CaMK II but not CaMK IV (Fig. 5*A* and Table 2). When liver sections were incubated with preimmune serum in the place of the primary antibody, no positive staining was observed (not shown). Measurement of the CaMK isoforms (I and II) by immunoblotting demonstrated that both small and large cholangiocyte lines express these isoforms (Fig. 5*B*). β-Actin was similarly expressed in small and large mouse cholangiocytes (Fig. 5*B*).

By real-time PCR, immortalized small and large cholangiocytes expressed the mRNA (measured as a ratio to GAPDH mRNA) for all the isoforms of CAMK I (α, γ, and δ) and CAMK II (α, δ, and γ) (Fig. 5*C*). Although CaMK I βI mRNA has been shown to be expressed by rat liver (63), we did not evaluate the expression of this isoform in mouse cholangiocytes, since the gene has not been cloned in mice yet.

Although immortalized small and large murine cholangiocytes express CaMK I and CaMK II, we only evaluated the effect of HTMT dimaleate on the phosphorylation of CaMK I in immortalized small cholangiocytes. The rationale for this experiment is based on the fact that: *1*) the HRH1 agonist HTMT dimaleate did not increase the proliferation of immortalized large cholangiocytes, thus excluding the need for evaluating the phosphorylation of CaMK I in large cholangiocytes, and *2*) the CaMK II isoform does not play a role in the regulation of small cholangiocyte proliferation, since the specific CaMK II inhibitor, AIP (30, 31), did not prevent the HTMT dimaleate-induced increase in small cholangiocyte proliferation (Fig. 3). The data show that HTMT dimaleate increased the phosphorylation of CaMK I in immortalized

Table 1. *Effect of the H1 agonist, HTMT dimaleate (10 μM), on $[Ca^{2+}]_i$ levels of immortalized small cholangiocytes*

	$[Ca^{2+}]_i$ Levels, nM
Basal	68.25±0.62
HTMT dimaleate	220.98±5.52*

Data are means ± SE; $n = 4$ experiments. $[Ca^{2+}]_i$, intracellular Ca^{2+} concentration; HTMT, histamine trifluoromethyl toluidine. Before Ca^{2+} measurements, immortalized small murine cholangiocytes were incubated for 1 h at 37°C to regenerate the membrane receptors damaged by isolation. Calcium fluorescence measurements were performed using fluo 3-AM (Molecular Probes) and a Fluoroskan Ascent FL (ThermoLabsystems) microplate reader equipped with three injectors (see MATERIALS AND METHODS). *$P < 0.05$ vs. basal value.

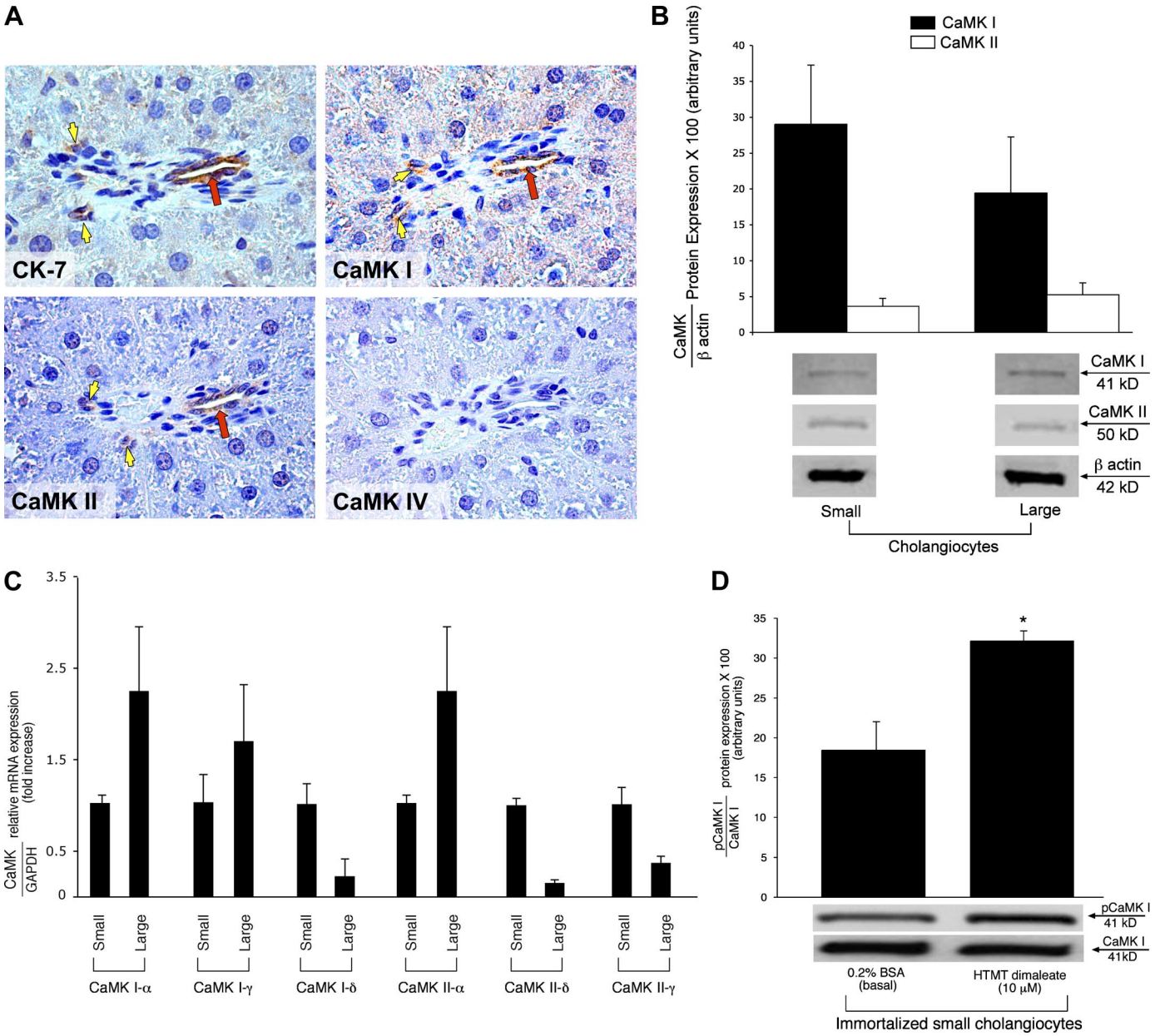

Fig. 5. *A*: representative micrographs of serial sections (4 μm thick; 3 slides evaluated for isoform) from normal mouse liver stained by immunohistochemistry for CK-7 and calmodulin-dependent protein kinase (CaMK) I, II, and IV. Both small (yellow arrowheads) and large (red arrows) bile ducts (specifically stained with CK-7) express CaMK I and CaMK II. Original magnification ×40. Measurement of the expression of CaMK I and CaMK II by immunoblots (*B*) and real-time PCR (*C*) in immortalized small and large murine cholangiocyte lines. We used rat brain (10 μg) as positive control for CaMK I, II, and IV. Data are means ± SE of 6 experiments. *D*: immunoblotting analysis of the phosphorylation of CaMK I in immortalized small cholangiocytes treated with HTMT or BSA (basal). Data are means ± SE of 6 immunoblots. $*P < 0.05$ compared with the basal value.

small cholangiocytes compared with small cholangiocytes treated with 0.2% BSA (basal) (Fig. 5*D*). Protein expression of total CaMK I was similar in immortalized small cholangiocytes treated with HTMT dimaleate or 0.2% BSA (basal) (Fig. 5*D*).

Knockdown of the CaMK I Gene Ablates the Stimulatory Effects of HTMT Dimaleate on Small Cholangiocyte Proliferation

Genetic knockdown of CaMK I was performed and confirmed by real-time PCR for CaMK I in all the clones. *Clone 22* (representative of all clones that we have evaluated for CaMK I message expression) had the highest degree of knockdown efficiency (~70%, Fig. 6*A*). Relative mRNA expression is shown in Fig. 6*A*. Following knockdown of the CaMK I mouse gene, HTMT dimaleate (10 μM) failed to increase the proliferation (evaluated by CellTiter Assay) (18) of immortalized small cholangiocytes compared with BSA-treated, transfected cells (Fig. 6*B*). HTMT dimaleate significantly increased the proliferation of small, empty vector-transfected cells compared with basal-treated empty vector-transfected cells (Fig. 6*B*). These data provide direct evidence for the role of CaMK

Table 2. *Immunohistochemical evaluation of the number of small and large bile ducts positive for CaMK I, CaMK II, and CaMK IV in serial liver sections from normal mice*

	No. of CaMK I-Positive Ducts	No. of CaMK II-Positive Ducts	No. of CaMK IV-Positive Ducts
Small bile ducts (<15 μm diameter)	62.4±4.0*	37.0±9.7	ND
Large bile ducts (>15 μm diameter)	70.59±5.7*	46.7±4.2	ND

Data are means ± SE of 5 cumulative values obtained from the evaluation of 10 different fields from 3 different sections (4 μm, 3 sections analyzed/isoform). CaMK, calmodulin-dependent protein kinase. *$P < 0.05$ vs. the corresponding no. of small and large bile ducts positive for CaMK II. ND, not detected.

I-dependent signaling in HRH1 modulation of small cholangiocyte growth.

Pharmacological and Genetic Evaluation of the Effect of HTMT Dimaleate on CREB Activation

We used both pharmacological inhibition and genetic manipulation to demonstrate the role of CaMK I in HRH1 regulation of CREB activity. In pharmacological experiments and utilizing nuclear extracts from immortalized small cholangiocytes treated with 0.2% BSA (basal) or HTMT dimaleate (10 μM in the absence or presence of W7), we evaluated the activity of the transcription factor CREB. CREB activity significantly increased in nuclear extracts from immortalized small cholangiocytes stimulated by HTMT dimaleate compared with basal treatment (Fig. 7*A*). Using pharmacological inhibition, we demonstrated that the activation of CREB by HTMT dimaleate was blocked by preincubation with W7 (Fig. 7*A*). For genetic manipulation, we used nuclear extracts from the previously created stable transfected CaMK I knockdown immortalized small cholangiocytes and demonstrated that CREB activity was increased in mock-transfected cell lines treated with HTMT dimaleate (Fig. 7*B*). Conversely, when the CaMK I knockdown cell line (70% knockdown efficiency) was used, the stimulatory effects of HTMT dimaleate on CREB activity were ablated (Fig. 7*B*).

DISCUSSION

Using immortalized small and large cholangiocyte lines (61), we have shown that small cholangiocytes (from small ducts) (61) proliferate in response to HTMT dimaleate by activation of the IP_3/Ca^{2+}/CaMK I/CREB signaling pathway. In contrast, immortalized large cholangiocytes [from large ducts (61)] do not proliferate in response to HTMT dimaleate. Consistent with the hypothesis that the HRH1 regulates small cholangiocyte proliferation, histamine (the endogenous agonist for the ligand) stimulation of small cholangiocyte proliferation was prevented by preincubation with terfenadine (a HRH1 antagonist) (33).

Small and large rat cholangiocytes differentially proliferate in a number of experimental models of cholestasis (6, 24, 35, 40–42, 46). Following BDL, large (but not small) cholangiocytes proliferate by activation of the cAMP-dependent signaling pathway (24, 35, 46). Small cholangiocytes (which are constitutively mitotically dormant) (24, 35, 46), de novo proliferate in pathological conditions associated with damage of large cholangiocytes (e.g., after CCl_4 administration) (40, 41). Feeding of taurocholic and taurolithocholic acid to rats increased proliferation of large cholangiocytes and induced the proliferation of small cholangiocytes (6). A number of theories have proposed regarding the function of small cholangiocytes (16, 35, 47, 60). Three-dimensional analysis of the architecture of Herring canals in normal and diseased human livers demonstrated that small cholangiocytes lining these canals constitute a functional stem cell population (60). We have also proposed that small cholangiocytes may be poorly differentiated primordial cells (35) in contrast to the more differentiated large cholangiocytes, which secrete water and electrolytes and

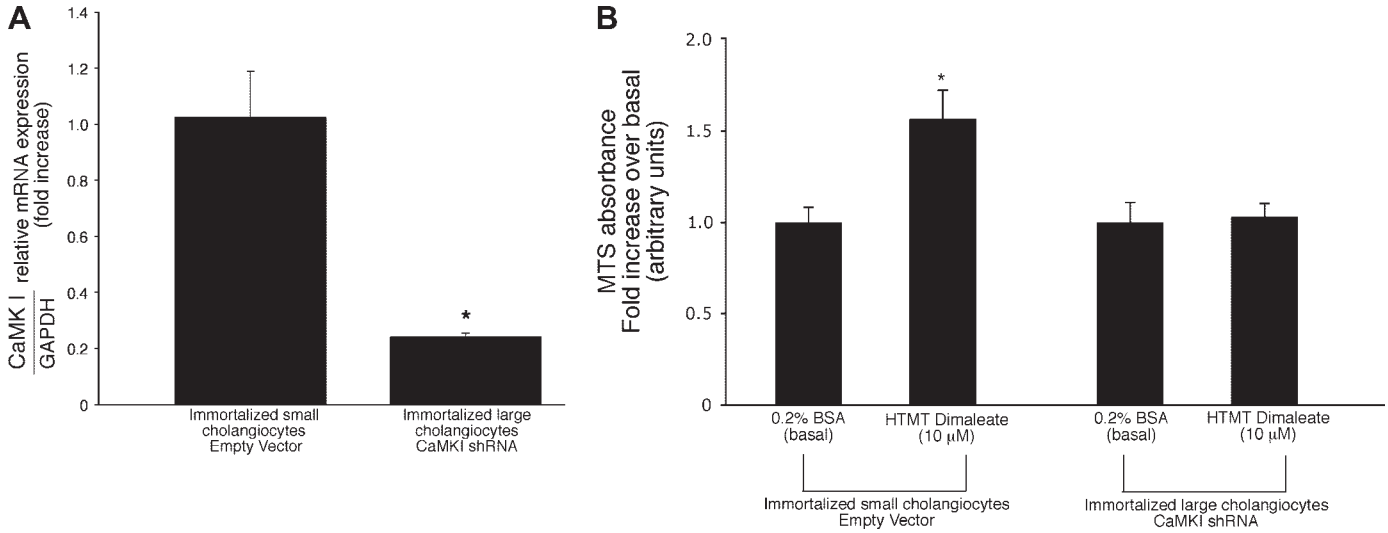

Fig. 6. *A*: characterization (by real-time PCR for CaMK I) of the short hairpin RNA (shRNA) clones revealed an ~70% knockdown in *clone 22*. Data are means ± SE of 3 experiments. *$P < 0.05$ compared with the corresponding value of immortalized small murine cholangiocytes transfected with empty shRNA vector. *B*: effect of HTMT dimaleate (10 μM) or 0.2% BSA (48 h of incubation) on the proliferation of CaMK I shRNA- or empty vector-transfected small murine cholangiocyte lines. Data are means ± SE of 12 experiments. *$P < 0.05$ compared with the corresponding basal value of immortalized small cholangiocytes transfected with empty shRNA vector.

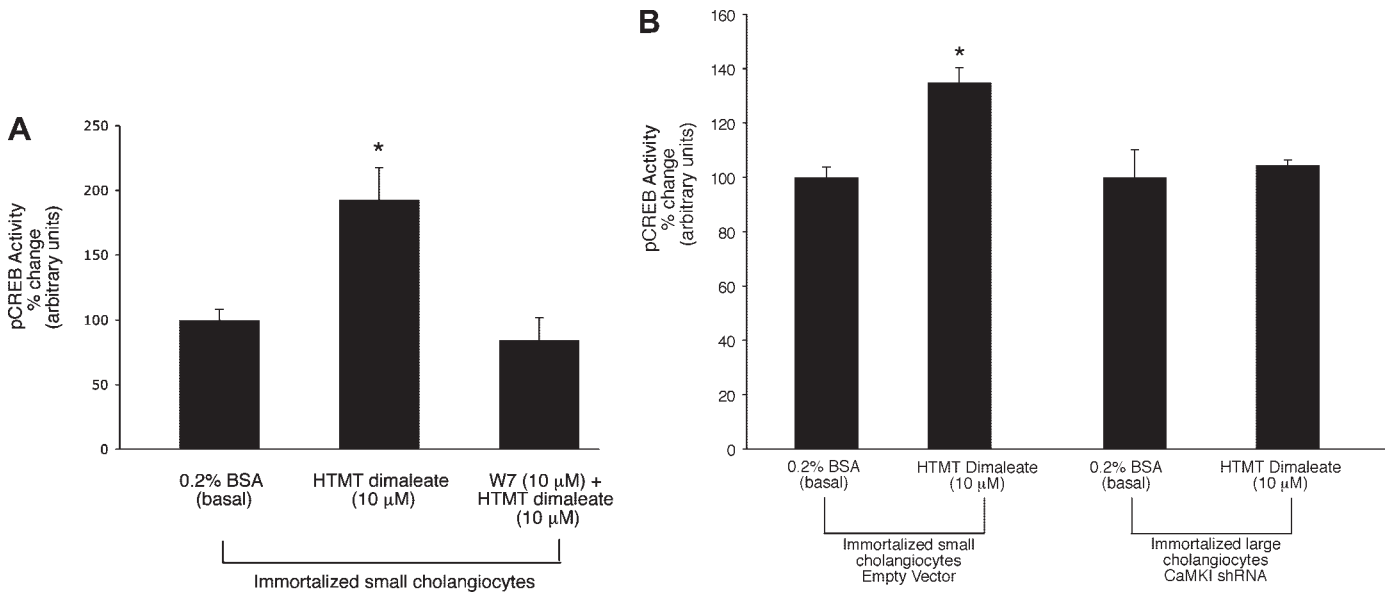

Fig. 7. *A*: measurement of phosphorylated cAMP-response element binding protein (CREB) activity in nuclear extracts from immortalized small cholangiocytes treated for 48 h at 37°C with 0.2% BSA (basal) or HTMT dimaleate (10 μM) in the absence or presence of W7 (10 μM). Data are means ± SE of 6 experiments. *$P < 0.05$ compared with all other groups. *B*: measurement of CREB activity in nuclear extract from mock-transfected or CaMK I knockdown immortalized small cholangiocytes treated with 0.2% BSA (basal) or HTMT dimaleate (10 μM) at 37°C for 48 h. Data are means ± SE of 3 experiments. *$P < 0.05$ compared with basal, empty vector.

proliferate in response to pathophysiological stimuli (3–5, 35, 41). Along this view, Masyuk et al. (47) have suggested that the differential proliferative capacity of different-sized cholangiocytes in response to various stimuli may be related not only to the nature of the stimulus but also to the heterogeneity of distributed proteins along the length of the biliary tree. However, despite these findings, the function of small cholangiocytes is undefined.

We provide further evidence that our immortalized small and large cholangiocytes (61) display features of freshly isolated cholangiocytes since: *1*) the size of small and large immortalized cholangiocytes was similar to that of freshly isolated small and large mouse cholangiocytes, and *2*) immortalized large cholangiocytes expressed the protein for secretin receptor, CFTR, and Cl^-/HCO_3^- AE2. Our findings, demonstrating that HRH1 are expressed by small and large bile ducts in normal mouse liver sections, immortalized small and large cholangiocyte lines, and freshly isolated small and large mouse cholangiocytes, further support the concept that immortalized small and large cholangiocytes retain phenotypes similar to freshly isolated cholangiocytes.

We next evaluated the effect of HTMT dimaleate on cholangiocyte proliferation and demonstrated that: *1*) HTMT dimaleate increases small but not large cholangiocyte proliferation, and *2*) the HTMT dimaleate-induced increase in small cholangiocyte proliferation was blocked by terfenadine, BAPTA/AM, and W7. Our studies, which provide the first evidence that small cholangiocyte proliferation (following activation of the HRH1) is induced by activation of the IP_3/CaMK I/CREB-dependent signaling pathway, have important clinical implications. Indeed, in patients with cystic fibrosis, it has been suggested that the IP_3/Ca^{2+}-dependent functional activity of small ducts (35) may compensate for the loss of large, cAMP-dependent cholangiocytes (2, 3, 5, 7, 24, 35, 40–42).

To explain why we have used different concentrations of HTMT dimaleate and histamine, we refer to a study that demonstrates that histamine has a much higher binding affinity compared with HTMT dimaleate (64). In this study (64), the authors used COS-1 cells (transiently transfected with AXOR35, a G protein-coupled receptor) to demonstrate competitive binding between histamine and numerous histamine receptor agonists and antagonists. The authors showed, with competitive [^{3}H]histamine binding, that histamine had a much greater affinity [inhibitory constant (K_i) = 17 ± 4 nM] compared with HTMT dimaleate (K_i = 1,229 ± 4 nM) to AXOR35 receptor-transfected membranes. This represents an ~100-fold difference between histamine and the HRH1 agonist, thus supporting our reasons and results obtained with our concentrations of 1 and 10 μM of histamine and HTMT dimaleate, respectively, on small cholangiocyte proliferation.

A possible explanation as to why there is a differential proliferative response of small and large cholangiocytes to HTMT dimaleate may be because of the selective increase in intracellular IP_3/Ca^{2+} by this cell subtype, and a subsequent activation of CAMK I. In agreement with this notion, we demonstrated that HTMT dimaleate did not increase intracellular cAMP levels in small cholangiocytes. Upregulation of HRH1 expression in small compared with large cholangiocytes may also explain why HTMT dimaleate stimulates only small cholangiocyte proliferation.

We next performed experiments aimed to pinpoint the specific CaMK isoform(s) involved in HTMT dimaleate stimulation of small cholangiocyte proliferation. We first demonstrated that both small and large cholangiocytes express all the isoforms of CaMK I (α, δ, and γ) and CaMK II (α, β, δ, and γ) but not CaMK IV. Although CaMK I β- I mRNA is present in rat liver (63), we did not evaluate the expression of this isoform in mouse cholangiocytes, since the gene has not been

cloned in mice yet. We demonstrated the key role of CaMK I in HRH1 modulation of small cholangiocyte growth, since HTMT dimaleate stimulation was associated with phosphorylation of CaMK I and blocked by gene silencing for this CaMK isoform. Although both small and large cholangiocytes express CaMK I and CaMK II, we evaluated the role of CaMK I based on the following observations. First, we excluded the role of CaMK II by demonstrating that the highly specific CaMK II inhibitor AIP (30, 31) did not block the HTMT dimaleate-induced increase of small cholangiocyte proliferation. Second, we did not evaluate the role of CaMK I in large murine cholangiocyte proliferation, since these cells do not respond to HTMT dimaleate. We did not evaluate the role of CaMK IV in the regulation of cholangiocyte proliferation, since this isoform was not expressed by these cells. Taken together, these findings demonstrated that HTMT dimaleate stimulation of small cholangiocyte proliferation depends on the phosphorylation of CaMK I.

We next performed experiments to evaluate if HTMT dimaleate stimulation of small cholangiocyte proliferation depends on CaMK I-dependent activation of CREB and demonstrated that HTMT dimaleate activation of small mouse cholangiocytes was associated with phosphorylation of CREB, which was blocked by W7 and CaMK I silencing. The ability of Ca^{2+} to regulate CREB activity involves phosphorylation of CREB by Ca^{2+}/CaMK (55, 62). CaMK I, II, and IV have been shown to phosphorylate CREB in vitro, providing evidence that each of these protein kinases may be a candidate for mediating the effects of Ca^{2+} on CREB activity (13, 14, 57).

Our current studies have important clinical implications, since a number of human liver diseases (e.g., primary biliary cirrhosis) are characterized by selective rather than diffuse proliferation or loss restricted to certain-sized ducts (4, 35). Our findings further support the concept that small and large cholangiocytes differentially respond to different stimuli (3, 35, 40–42). Indeed, depending on the need of the liver, either growth-promoting receptor is activated (like HRH1 or HRH2), or growth-inhibiting (such as HRH3 or HRH4) receptors are "switched on." This fine balance exists to regulate the function(s) of cholangiocytes in the modulation of liver diseases. The regulation of the biogenic amine histamine (via 4 independent receptors) may be important in this balance of heterogeneous proliferation and loss in liver disease management.

ACKNOWLEDGMENTS

We acknowledge the Texas A&M Health Science Center Microscopy Imaging Center for assistance with the confocal microscopy imaging. We thank Meg Chrisler and Glen Cryer, Division of Scientific Publications, Scott & White, for assistance in editing the manuscript.

GRANTS

The study was supported by the Dr. Nicholas C. Hightower Centennial Chair of Gastroenterology from Scott & White, the Veterans Affairs (VA) Research Scholar Award, a VA Merit Award to G. Alpini, a K01 National Institutes of Health (NIH) grant award (DK-078532) to S. DeMorrow, a grant award from Health and Labour Sciences Research, grants for the Research on Measures for Intractable Diseases from the Ministry of Health, Labour, and Welfare of Japan, by a Grant-in-Aid for Scientific Research C (19590744) from Japan Society for the Promotion of Science to Y. Ueno, by NIH Grant HL-68838-01 to D. Dostal, by Ministero dell'Istruzione, dell'Università e della Ricerca Grants 2005067975_004 (to M. Marzioni), 2005069739_002 (to P. Onori), and 2005067975_001, and by faculty funds from the University of Rome "La Sapienza" to E. Gaudio.

REFERENCES

1. **Alpini G, Baiocchi L, Glaser S, Ueno Y, Marzioni M, Francis H, Phinizy JL, Angelico M, LeSage G.** Ursodeoxycholate and tauroursodeoxycholate inhibit cholangiocyte growth and secretion of BDL rats through activation of PKC alpha. *Hepatology* 35: 1041–1052, 2002.
2. **Alpini G, Glaser S, Robertson W, Rodgers RE, Phinizy JL, Lasater J, LeSage G.** Large but not small intrahepatic bile ducts are involved in secretin-regulated ductal bile secretion. *Am J Physiol Gastrointest Liver Physiol* 272: G1064–G1074, 1997.
3. **Alpini G, Glaser S, Ueno Y, Pham L, Podila PV, Caligiuri A, LeSage G, LaRusso NF.** Heterogeneity of the proliferative capacity of rat cholangiocytes after bile duct ligation. *Am J Physiol Gastrointest Liver Physiol* 274: G767–G775, 1998.
4. **Alpini G, Prall RT, LaRusso NF.** The pathobiology of biliary epithelia. In: *The Liver; Biology & Pathobiology* (4th ed.), edited by Arias IM, Boyer JL, Chisari FV, Fausto N, Jakoby W, Schachter D, and Shafritz DA. Philadelphia, PA: Williams & Wilkins, 2001, p. 421–435.
5. **Alpini G, Roberts S, Kuntz SM, Ueno Y, Gubba S, Podila PV, LeSage G, LaRusso NF.** Morphological, molecular, and functional heterogeneity of cholangiocytes from normal rat liver. *Gastroenterology* 110: 1636–1643, 1996.
6. **Alpini G, Ueno Y, Glaser S, Marzioni M, Phinizy JL, Francis H, LeSage G.** Bile acid feeding increased proliferative activity and apical bile acid transporter expression in both small and large rat cholangiocytes. *Hepatology* 34: 868–876, 2001.
7. **Alpini G, Ulrich C, Roberts S, Phillips JO, Ueno Y, Podila PV, Colegio O, LeSage G, Miller LJ, LaRusso NF.** Molecular and functional heterogeneity of cholangiocytes from rat liver after bile duct ligation. *Am J Physiol Gastrointest Liver Physiol* 272: G289–G297, 1997.
8. **Alvaro D, Mancino MG, Glaser S, Gaudio E, Marzioni M, Francis H, Alpini G.** Proliferating cholangiocytes: a neuroendocrine compartment in the diseased liver. *Gastroenterology* 132: 415–431, 2006.
9. **Aromolaran AA, Blatter LA.** Modulation of intracellular Ca^{2+} release and capacitative Ca^{2+} entry by CaMKII inhibitors in bovine vascular endothelial cells. *Am J Physiol Cell Physiol* 289: C1426–C1436, 2005.
10. **Banales JM, Arenas F, Rodriguez-Ortigosa CM, Saez E, Uriarte I, Doctor RB, Prieto J, Medina JF.** Bicarbonate-rich choleresis induced by secretin in normal rat is taurocholate-dependent and involves AE2 anion exchanger. *Hepatology* 43: 266–275, 2006.
11. **Benedetti A, Bassotti C, Rapino K, Marucci L, Jezequel AM.** A morphometric study of the epithelium lining the rat intrahepatic biliary tree. *J Hepatol* 24: 335–342, 1996.
12. **Braun AP, Schulman H.** The multifunctional calcium/calmodulin-dependent protein kinase: from form to function. *Annu Rev Physiol* 57: 417–445, 1995.
13. **Cruzalegui FH, Means AR.** Biochemical characterization of the multifunctional Ca^{2+}/calmodulin-dependent protein kinase type IV expressed in insect cells. *J Biol Chem* 268: 26171–26178, 1993.
14. **Dash PK, Karl KA, Colicos MA, Prywes R, Kandel ER.** cAMP response element-binding protein is activated by Ca^{2+}/calmodulin- as well as cAMP-dependent protein kinase. *Proc Natl Acad Sci USA* 88: 5061–5065, 1991.
15. **Dickenson JM.** Stimulation of protein kinase B and p70 S6 Kinase by the histamine H1 receptor in DDT1MF-2 smooth muscle cells. *Br J Pharmacol* 135: 1967–1976, 2002.
16. **Dofour JF.** Biliary epithelial cells. In: *Textbook of Hepatology: From Basic Science to Clinical Practice*, edited by Rodés J, Benhamou J-P, Blei A, Reichen J, and Rizzetto M. Oxford, UK: Blackwell, 2007, p. 52–58.
17. **Enslen H, Sun P, Brickey D, Soderling SH, Klamo E, Soderling TR.** Characterization of Ca^{2+}/calmodulin-dependent protein kinase IV. Role in transcriptional regulation. *J Biol Chem* 269: 15520–15527, 1994.
18. **Fava G, Marucci L, Glaser S, Francis H, De Morrow S, Benedetti A, Alvaro D, Venter J, Meininger C, Patel T, Taffetani S, Marzioni M, Summers R, Reichenbach R, Alpini G.** gamma-Aminobutyric acid inhibits cholangiocarcinoma growth by cyclic AMP-dependent regulation of the protein kinase A/extracellular signal-regulated kinase 1/2 pathway. *Cancer Res* 65: 11437–11446, 2005.
19. **Fava G, Ueno Y, Glaser S, Francis H, DeMorrow S, Marucci L, Marzioni M, Benedetti A, Venter J, Vaculin B, Vaculin S, Alpini G.** Thyroid hormone inhibits biliary growth in bile duct-ligated rats by PLC/$IP_{(3)}$/$Ca^{(2+)}$-dependent downregulation of SRC/ERK1/2. *Am J Physiol Cell Physiol* 292: C1467–C1475, 2007.

20. **Francis H, Franchitto A, Ueno Y, Glaser S, DeMorrow S, Venter J, Gaudio E, Alvaro D, Fava G, Marzioni M, Vaculin B, Alpini G.** H3 histamine receptor agonist inhibits biliary growth of BDL rats by down-regulation of the cAMP-dependent PKA/ERK1/2/ELK-1 pathway. *Lab Invest* 87: 473–487, 2007.
21. **Francis H, Glaser S, Ueno Y, LeSage G, Marucci L, Benedetti A, Taffetani S, Marzioni M, Alvaro D, Venter J, Reichenbach R, Fava G, Phinizy JL, Alpini G.** cAMP stimulates the secretory and proliferative capacity of the rat intrahepatic biliary epithelium through changes in the PKA/Src/MEK/ERK1/2 pathway. *J Hepatol* 41: 528–537, 2004.
22. **Gaudio E, Barbaro B, Alvaro D, Glaser S, Francis H, Ueno Y, Meininger CJ, Franchitto A, Onori P, Marzioni M, Taffetani S, Fava G, Stoica G, Venter J, Reichenbach R, De Morrow S, Summers R, Alpini G.** Vascular endothelial growth factor stimulates rat cholangiocyte proliferation via an autocrine mechanism. *Gastroenterology* 130: 1270–1282, 2006.
23. **Glaser S, Benedetti A, Marucci L, Alvaro D, Baiocchi L, Kanno N, Caligiuri A, Phinizy JL, Chowdhury U, Papa E, LeSage G, Alpini G.** Gastrin inhibits cholangiocyte growth in bile duct-ligated rats by interaction with cholecystokinin-B/Gastrin receptors via D-myo-inositol 1,4,5-triphosphate-, $Ca^{(2+)}$-, and protein kinase C alpha-dependent mechanisms. *Hepatology* 32: 17–25, 2000.
24. **Glaser S, Francis H, DeMorrow S, LeSage G, Fava G, Marzioni M, Venter J, Alpini G.** Heterogeneity of the intrahepatic biliary epithelium. *World J Gastroenterol* 12: 3523–3536, 2006.
25. **Glaser S, Pierce L, Rao A, Gaudio E, Franchitto A, Onori P, Venter J, Francis H, Vaculin B, Vaculin S, DeMorrow S, Kelley K, Perry B, McNeal M, Alpini G.** Morphological and functional heterogeneity of the murine intrahepatic biliary epithelium (Abstract). *Hepatology* 46: A220, 2007.
26. **Glaser S, Ueno Y, DeMorrow S, Chiasson VL, Katki KA, Venter J, Francis HL, Dickerson IM, Dipette DJ, Supowit SC, Alpini G.** Knockout of alpha-calcitonin gene-related peptide reduces cholangiocyte proliferation in bile duct ligated mice. *Lab Invest* 87: 914–926, 2007.
27. **Harrison SM, Bers DM.** The effect of temperature and ionic strength on the apparent Ca-affinity of EGTA and the analogous Ca-chelators BAPTA and dibromo-BAPTA. *Biochim Biophys Acta* 925: 133–143, 1987.
28. **Hook SS, Means AR.** $Ca^{(2+)}$/CaM-dependent kinases: from activation to function. *Annu Rev Pharmacol Toxicol* 41: 471–505, 2001.
29. **Hook SS, Means AR.** $Ca^{(2+)}$/CaM-dependent kinases: from activation to function. *Annu Rev Pharmacol Toxicol* 41: 471–505, 2001.
30. **Ishida A, Fujisawa H.** Stabilization of calmodulin-dependent protein kinase II through the autoinhibitory domain. *J Biol Chem* 270: 2163–2170, 1995.
31. **Ishida A, Kameshita I, Okuno S, Kitani T, Fujisawa H.** A novel highly specific and potent inhibitor of calmodulin-dependent protein kinase II. *Biochem Biophys Res Commun* 212: 806–812, 1995.
32. **Ishii M, Vroman B, LaRusso NF.** Isolation and morphologic characterization of bile duct epithelial cells from normal rat liver. *Gastroenterology* 97: 1236–1247, 1989.
33. **Jangi SM, Diaz-Perez JL, Ochoa-Lizarralde B, Martin-Ruiz I, Asumendi A, Perez-Yarza G, Gardeazabal J, Diaz-Ramon JL, Boyano MD.** H1 histamine receptor antagonists induce genotoxic and caspase-2-dependent apoptosis in human melanoma cells. *Carcinogenesis* 27: 1787–1796, 2006.
34. **Kanno N, LeSage G, Glaser S, Alpini G.** Regulation of cholangiocyte bicarbonate secretion. *Am J Physiol Gastrointest Liver Physiol* 281: G612–G625, 2001.
35. **Kanno N, LeSage G, Glaser S, Alvaro D, Alpini G.** Functional heterogeneity of the intrahepatic biliary epithelium. *Hepatology* 31: 555–561, 2000.
36. **Kassack M, Hofgen B, Lehmann J, Eckstein N, Quillan J, Sadee W.** Functional screening of G protein-coupled receptors by measuring intracellular calcium with a fluorescence microplate reader. *J Biomol Screening* 7: 233–246, 2002.
37. **Kato A, Gores GJ, LaRusso NF.** Secretin stimulates exocytosis in isolated bile duct epithelial cells by a cyclic AMP-mediated mechanism. *J Biol Chem* 267: 15523–15529, 1992.
38. **Lazaridis KN, Strazzabosco M, LaRusso NF.** The cholangiopathies: disorders of biliary epithelia. *Gastroenterology* 127: 1565–1577, 2004.
39. **LeSage G, Alvaro D, Glaser S, Francis H, Marucci L, Roskams T, Phinizy JL, Marzioni M, Benedetti A, Taffetani S, Barbaro B, Fava G, Ueno Y, Alpini G.** Alpha-1 adrenergic receptor agonists modulate ductal secretion of BDL rats via $Ca^{(2+)}$- and PKC-dependent stimulation of cAMP. *Hepatology* 40: 1116–1127, 2004.
40. **LeSage G, Benedetti A, Glaser S, Marucci L, Tretjak Z, Caligiuri A, Rodgers R, Phinizy JL, Baiocchi L, Francis H, Lasater J, Ugili L, Alpini G.** Acute carbon tetrachloride feeding selectively damages large, but not small, cholangiocytes from normal rat liver. *Hepatology* 29: 307–319, 1999.
41. **LeSage G, Glaser S, Marucci L, Benedetti A, Phinizy JL, Rodgers R, Caligiuri A, Papa E, Tretjak Z, Jezequel AM, Holcomb LA, Alpini G.** Acute carbon tetrachloride feeding induces damage of large but not small cholangiocytes from BDL rat liver. *Am J Physiol Gastrointest Liver Physiol* 276: G1289–G1301, 1999.
42. **LeSage G, Glaser S, Ueno Y, Alvaro D, Baiocchi L, Kanno N, Phinizy JL, Francis H, Alpini G.** Regression of cholangiocyte proliferation after cessation of ANIT feeding is coupled with increased apoptosis. *Am J Physiol Gastrointest Liver Physiol* 281: G182–G190, 2001.
43. **Lim HD, van Rijn RM, Ling P, Bakker RA, Thurmond RL, Leurs R.** Evaluation of histamine H1-, H2-, and H3-receptor ligands at the human histamine H4 receptor: identification of 4-methylhistamine as the first potent and selective H4 receptor agonist. *J Pharmacol Exp Ther* 314: 1310–1321, 2005.
44. **Martinez-Anso E, Castillo JE, Diez J, Medina JF, Prieto J.** Immunohistochemical detection of chloride/bicarbonate anion exchangers in human liver. *Hepatology* 19: 1400–1406, 1994.
45. **Marzioni M, Alpini G, Saccomanno S, de Minicis S, Glaser S, Francis H, Trozzi L, Venter J, Orlando F, Fava G, Candelaresi C, Macarri G, Benedetti A.** Endogenous opioids modulate the growth of the biliary tree in the course of cholestasis. *Gastroenterology* 130: 1831–1847, 2006.
46. **Marzioni M, Glaser S, Francis H, Phinizy JL, LeSage G, Alpini G.** Functional heterogeneity of cholangiocytes. *Semin Liver Dis* 22: 227–240, 2002.
47. **Masyuk TV, Ritman EL, LaRusso NF.** Quantitative assessment of the rat intrahepatic biliary system by three-dimensional reconstruction. *Am J Pathol* 158: 2079–2088, 2001.
48. **McGill JM, Yen MS, Basavappa S, Mangel AW, Kwiatkowski AP.** ATP-activated chloride permeability in biliary epithelial cells is regulated by calmodulin-dependent protein kinase II. *Biochem Biophys Res Commun* 208: 457–462, 1995.
49. **Mitsuhashi M, Mitsuhashi T, Payan D.** Multiple signaling pathways of histamine H2 receptors (Identification of an H2 receptor-dependent Ca^{2+} mobilization pathway in human HL-60 promyelocytic leukemia cells). *J Biol Chem* 264: 18356–18362, 1989.
50. **Nguyen T, Shapiro DA, George SR, Setola V, Lee DK, Cheng R, Rauser L, Lee SP, Lynch KR, Roth BL, O'Dowd BF.** Discovery of a novel member of the histamine receptor family. *Mol Pharmacol* 59: 427–433, 2001.
51. **Pérez GJ, Bonev AD, Nelson MT.** Micromolar Ca^{2+} from sparks activates Ca^{2+}-sensitive K^+ channels in rat cerebral artery smooth muscle. *Am J Physiol Cell Physiol* 281: C1769–C1775, 2001.
52. **Polimeno L, Azzarone A, Zeng QH, Panella C, Subbotin V, Carr B, Bouzahzah B, Francavilla A, Starzl TE.** Cell proliferation and oncogene expression after bile duct ligation in the rat: evidence of a specific growth effect on bile duct cells. *Hepatology* 21: 1070–1078, 1995.
53. **Repka-Ramirez MS.** New concepts of histamine receptors and actions. *Curr Allergy Asthma Rep* 3: 227–231, 2003.
54. **Rossi NF, Schrier RW.** Anti-calmodulin agents affect osmotic and angiotensin II-induced vasopressin release. *Am J Physiol Endocrinol Metab* 256: E516–E523, 1989.
55. **Sato K, Suematsu A, Nakashima T, Takemoto-Kimura S, Aoki K, Morishita Y, Asahara H, Ohya K, Yamaguchi A, Takai T, Kodama T, Chatila TA, Bito H, Takayanagi H.** Regulation of osteoclast differentiation and function by the CaMK-CREB pathway. *Nat Med* 12: 1410–1416, 2006.
56. **Shayo C, Fernandez N, Legnazzi BL, Monczor F, Mladovan A, Baldi A, Davio C.** Histamine H2 receptor desensitization: involvement of a select array of G protein-coupled receptor kinases. *Mol Pharmacol* 60: 1049–1056, 2001.
57. **Sheng M, Thompson MA, Greenberg ME.** CREB: a $Ca^{(2+)}$-regulated transcription factor phosphorylated by calmodulin-dependent kinases. *Science* 252: 1427–1430, 1991.
58. **Taffetani S, Glaser S, Francis H, DeMorrow S, Ueno Y, Alvaro D, Marucci L, Marzioni M, Fava G, Venter J, Vaculin S, Vaculin B, Lam IP, Lee VH, Gaudio E, Carpino G, Benedetti A, Alpini G.** Prolactin stimulates the proliferation of normal female cholangiocytes by differential regulation of Ca^{2+}-dependent PKC isoforms (Abstract). *BMC Physiol* 7: 6, 2007.

59. **Tanaka T, Ohmura T, Hidaka H.** Calmodulin antagonists' binding sites on calmodulin. *Pharmacology* 26: 249–257, 1983.
60. **Theise ND, Saxena R, Portmann BC, Thung SN, Yee H, Chiriboga L, Kumar A, Crawford JM.** The canals of Hering and hepatic stem cells in humans. *Hepatology* 30: 1425–1433, 1999.
61. **Ueno Y, Alpini G, Yahagi K, Kanno N, Moritoki Y, Fukushima K, Glaser S, LeSage G, Shimosegawa T.** Evaluation of differential gene expression by microarray analysis in small and large cholangiocytes isolated from normal mice. *Liver Int* 23: 449–459, 2003.
62. **Wayman GA, Impey S, Marks D, Saneyoshi T, Grant WF, Derkach V, Soderling TR.** Activity-dependent dendritic arborization mediated by CaM-kinase I activation and enhanced CREB-dependent transcription of Wnt-2. *Neuron* 50: 897–909, 2006.
63. **Yokokura H, Terada O, Naito Y, Hidaka H.** Isolation and comparison of rat cDNAs encoding Ca^{2+}/calmodulin-dependent protein kinase I isoforms 1. *Biochim Biophys Acta* 1338: 8–12, 1997.
64. **Zhu Y, Michalovich D, Wu H, Tan KB, Dytko GM, Mannan IJ, Boyce R, Alston J, Tierney LA, Li X, Herrity NC, Vawter L, Sarau HM, Ames RS, Davenport CM, Hieble JP, Wilson S, Bergsma DJ, Fitzgerald LR.** Cloning, expression, and pharmacological characterization of a novel human histamine receptor. *Mol Pharmacol* 59: 434–441, 2001.